Int J Adv Manuf Technol (2014) 73:973–980
DOI 10.1007/s00170-014-5805-8

ORIGINAL ARTICLE

Oil whip-induced wear in journal bearings

Kjell G. Robbersmyr · Herman Olsen · Hamid Reza Karimi · Kristian Tønder

Received: 15 September 2013 / Accepted: 24 March 2014 / Published online: 10 May 2014

Abstract This paper investigates the effect of oil whirl and oil whip in fluid film radial bearings due to possible metallic contact. The degree of metallic contact and thereby wear and tear between rotating shafts and bearing bushes is assessed by measuring electric currents through the oil film. The current as well as the voltage varied in accordance with the contact ratio between the shaft and bush in the fluid film radial bearing. The gauge signal thus indicates the degree of metallic contact based on the thickness of the oil film in the load zone. Some experimental results are provided to illustrate that at low normalised loads involving oil whirl and oil whip, no electric current is detected, while high levels of electric current are registered at high load levels when no oil whirl or oil whip occurred. It is therefore concluded that at low loads, oil whirl and oil whip have little influence on wear and tear in a journal bearing.

Keywords Oil whirl · Oil whip · Fluid film radial bearings

K. G. Robbersmyr (✉) · H. R. Karimi
Faculty of Engineering and Science, Department of Engineering Sciences, Mechatronics, University of Agder, 4886 Grimstad, Norway
e-mail: kjell.g.robbersmyr@uia.no

H. Olsen
Faculty of Technology, Department of Mechanical and Logistical Engineering, Sør-Trøndelag University College, 7005 Trondheim, Norway

K. Tønder
Department of Product Development and Material Engineering, Norwegian University of Science and Technology, 7491 Trondheim, Norway

1 Introduction

Oil-induced shaft vibrations in journal bearings have often been regarded as being a problem. These rotations or vibrations, known as oil whirl and oil whip, are self-excited phenomena transferring energy to the vibration motion essentially at all rotation frequencies. The mechanism behind oil whirl and oil whip is outlined and discussed in detail in [1–4]. In [5], it is reported that pure rotational motion of the shaft becomes unstable and then the whirl regime will be stable. When the rotational speed is increasing, the whirl smoothly transforms into whip, and at a certain speed, the whip may disappear and the second-mode whirl starts again. An analysis of oil whirl and oil whip in journal bearing lubrication is also described in [6–10]. For instance, Schweizer [6] investigated the occurring oil whirl/whip effects for a Laval rotor by means of run-up simulations. In [7], the authors presented an analysis method for the dynamic behaviour of a rotating system under the oil whirl and oil whip phenomenon, considering the influence of unbalance, rotor arrangement and bearing parameters on the instability threshold. Moreover, in [10], an experimental study was performed to investigate the fluttering characteristics of a tilting pad journal bearing with the variation of supply oil flow rate, shaft speed and bearing load.

Recently, in [11], an effective method is proposed to observe the coexistence of oil whip and dry whip using a full Hilbert spectrum. The authors in [12] investigated a Laval (Jeffcott) rotor, which is symmetrically supported in full-floating ring bearings, and investigated the occurring oil whirl/whip effects by means of run-up simulations. However, in [13], the dynamic behaviour of a rotating system is studied under the oil whirl and oil whip phenomenon, considering the influence of unbalance, rotor arrangement (vertical or

horizontal rotor) and bearing parameters on the instability threshold. Also, the authors in [14] investigated the fluttering characteristics of the upper unloaded pads in a tilting pad journal bearing experimentally.

Oil whirl appears in practice at a frequency located just under the shaft's half rotation frequency. When the shaft rotation is increased by twice the critical rotational speed or higher, the oil whirl becomes an unstable oil whip. Oil whip always takes place at a frequency equivalent to the shaft's critical rotational speed, resulting in a vibration response that 'whips' the fluid film. A visual inspection through a bearing bush of plexiglass and using coloured oil shows that the oil film disappears periodically implying a loss of bearing ability.

The objective of the present work is to investigate the mechanism of oil whirl and whip in fluid film bearings. The problems caused by oil whirl and whip are highlighted. Moreover, frequency analysis of a shaft exhibiting oil whirl is carried out.

This paper is organised as follows. Section 2 describes the testing setup. Section 3 presents results from vibration monitoring and from measuring the electric current in the oil film between the bearing surfaces. In Section 4, the results are discussed and some remarks are provided. Finally, some concluding remarks are given in Section 5.

2 Measurement setup

The testing setup of shaft and bearing is identical to the setup utilised and explained in [1]. In Fig. 1, the steel bearing used during the tests is displayed. The shaft is supported by two bearings, one being a large-diameter shaft section in a steel sleeve, the other a 'dry' bronze plain bearing of much smaller diameter. The lubricating oil is drained from the bearing and pumped back to the reservoir and then reused in the bearing (see Fig. 1). One rotor mass is used, and the critical shaft speed is measured to be 2,400 rpm.

On the calculation of the forces in the fluid film bearing, oil whirl gives rise to a centripetal acceleration due to the shaft orbital motion within the bearing. The centripetal force is given by

$$F_{\text{centripetal}} = e(k\omega)^2 \tag{1}$$

where

e eccentricity of the shaft [m]
k constant (0.46–0.49)
ω angular velocity [rad/s]

Increased centripetal force results in increased pressure forces in the oil film increasing the tangential force, thereby maintaining and increasing the oil whirl.

Vibration monitoring using frequency analysis was undertaken in order to reveal oil whirl and oil whip, and measurements of electrical current through the oil film are taken in the bearing surfaces:

- *Vibration check*: Non-contact proximity transducers are used to monitor shaft motion. Registration of the rotations is achieved through use of a portable data collector having a frequency analysis module (Microlog). The measurements are transferred to the PC via cable, and analyses are completed through use of the PRISM4 frequency analysis programme [15]. The portable data collector with frequency analysis module is shown in Fig. 2a.

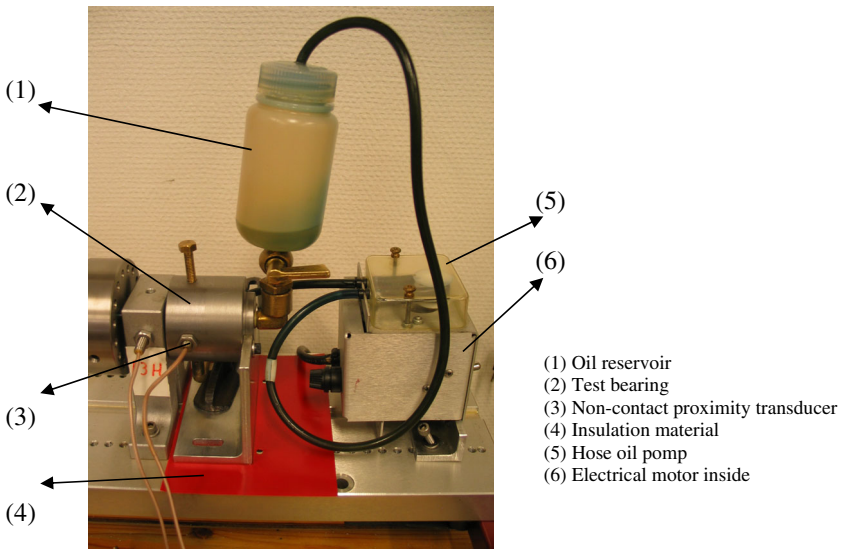

Fig. 1 Fluid film bearing with lubricating oil reservoir. *(1)* indicates oil reservoir, *(2)* test bearing, *(3)* non-contact proximity transducer, *(4)* insulation material, *(5)* hose oil pomp, and *(6)* electrical motor inside

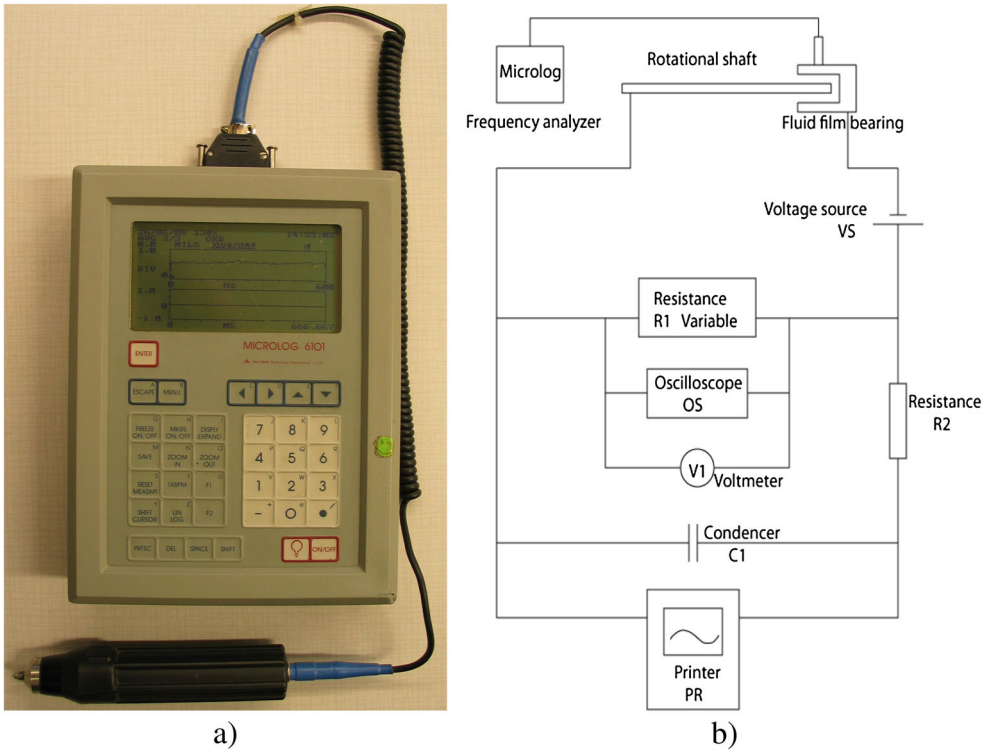

Fig. 2 **a** Portable data collector with frequency analysis module. **b** Connector diagram for measuring electric current/ metallic contact between bearing surfaces in the journal bearing

The total vibration level at a gauge point is represented by the RMS of the various components of the spectrum,

$$s_{overall} = \sqrt{\sum_{i=1}^{n} S_i^2} \text{ [microns]}$$

in which s_i is the magnitude of ith frequency component.

Results from the frequency analysis may be presented as waterfall plots.

- *Measuring electric current*: In order to measure any disruptions in the oil film with corresponding metallic contact in the bearing surfaces, electric currents are transmitted (less than 0.1 A) through the bearing. Unfiltered registrations of such currents visualised on the oscilloscope often show quite low contact time (microseconds) under moderate radial loads. The oscilloscope measurements showed that the average signal is produced from brief electrical currents: contact/no contact. Frequent contacts thus produce high average electrical currents. Likewise, low average electrical current is caused by less frequent contact peaks. A measurement setup without filtering will suffer considerable interference. In order to lower interference, a low-pass filter (RC filter), in parallel with a variable resistance, is used [16, 17]. The corresponding connector diagram is shown in Fig. 2b. This connection produces a filter with an upper limit frequency: 0.08 Hz with 3-dB reduction.

Equipment and components shown in Fig. 2b contain the following data:

• Microlog	Frequency analyser/data collector, Palomar Microlog 6101
• VS: Voltage source	GW Laboratory DC Power Supply GPR-3030; adjusted value equals 2.7 V
• R1: Resistance	Adjusted value equals 40 Ω (variable 0–40 Ω)
• R2: Resistance	Constant value equals R=9.6 MΩ
• OS: Oscilloscope	SS-5702 Oscilloscope DC–20MHz
• V1: Voltmeter	Philips PM97, 50MHz scopemeter
• C1: Condenser	Constant value equals C=204 nF
• PR: Printer	HP 320 Dual Channel DC Amplifier Recorder
• Software:	Prism4, frequency analysis programme for Windows

The tests were completed by altering both the load and rotational speed of the shaft. The shaft was loaded radially in a vertical direction, by means of an additional 'dry' bronze plain bearing connected to a very flexible spring with spring stiffness $k_{\text{spring}} = 114N/m$ and adjustment screw, with forces varying from 0 to 25 N. The rotational frequency was varied between 25 and 192 Hz. A proximity transducer was used for measurement of the radial horizontal peak to peak shaft movement within the bearing.

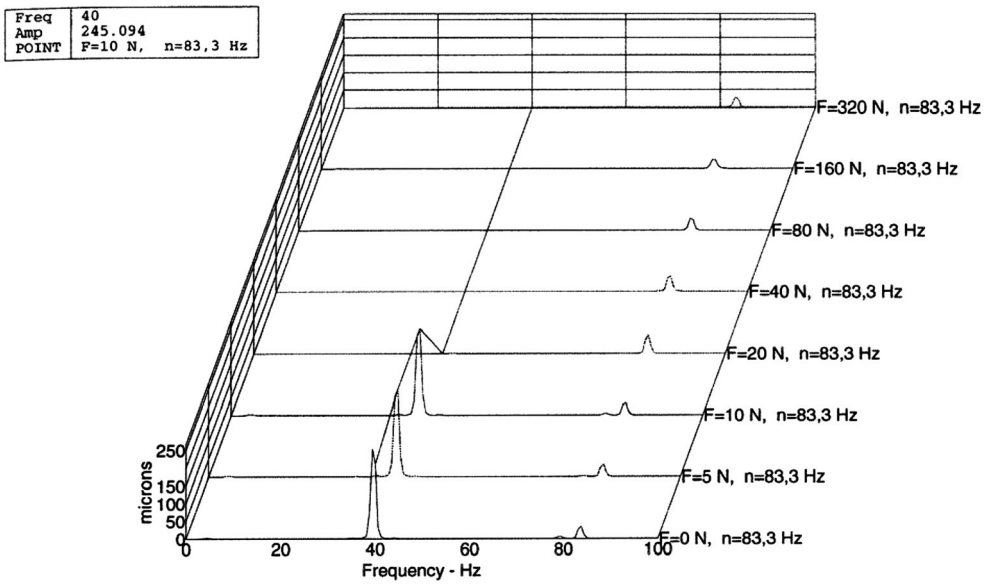

Fig. 3 Vibration level measurement

3 Measurement results

Results from vibration monitoring (frequency analysis) and from measuring the electric current in the oil film between the bearing surfaces are shown below:

Vibration level Figure 3 shows an example of measurements from the frequency analysis presented as a waterfall plot. The plot represents a rotational speed of 5,000 r/min, with loads fluctuating from 0 to 320 N. The figure shows that oil whirl arose at a frequency of 40 Hz for the three lowest radial loads. This is 48 % of the actual rotational frequency of the shaft (83.3 Hz).

At loads up to 10 N, all measurements show oil whirl and oil whip at shaft rotational speeds lower and higher than 5,000 r/min, respectively. The frequency peak representing oil whirl is always very close to half the shaft rotational frequency (47–49 %). When the rotational speed exceeds

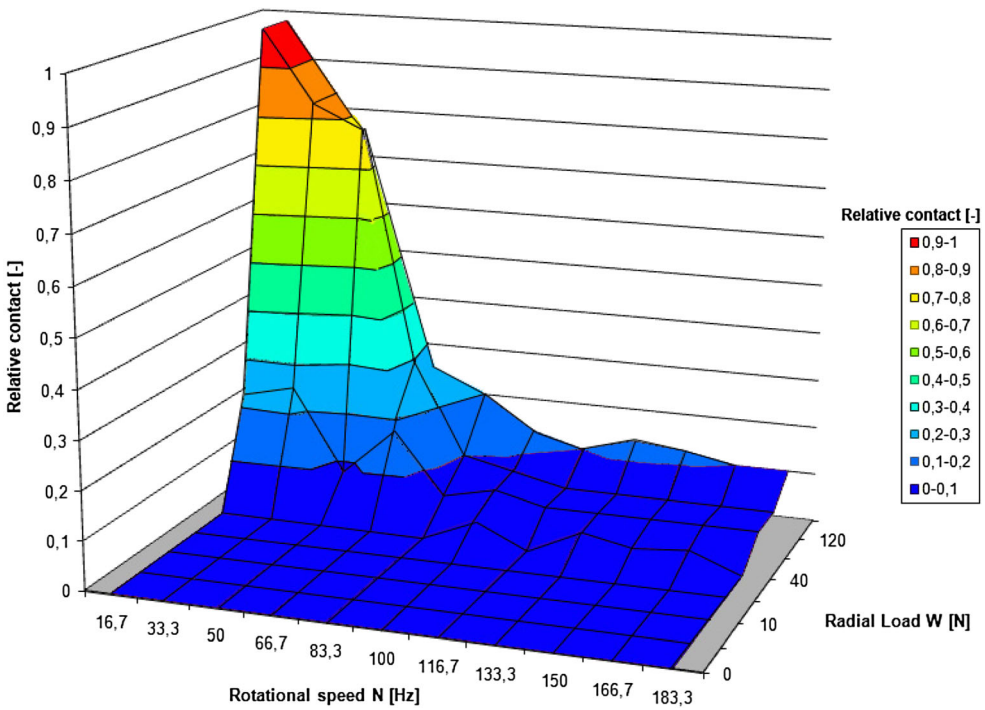

Fig. 4 Relative electric current

twice the critical rotational speed level, the oil whirl becomes oil whip and is locked at 40 Hz, which is the critical rotational frequency of the shaft.

Measuring the electric current Figure 4 shows the results from the measurements of the mean current in the bearing, where the relative contact is a relative motion between the mating surfaces of a plain bearing. A total of 88 mean current measurements with different rotational speeds and radial loads have been taken.

For the entire rotational speed spectrum, there was little or no electric current (metallic contact) between the bearing surfaces in the fluid film bearing for radial loads up to 20 N. On the other hand, there is a noticeable contact increase at low rotational speed and high loads and an increase of up to almost full contact at approximately 16.7 Hz rotational frequency at a load of 120 N. In addition, some interference/unrealistic values were observed at loads of 120 N and rotational speeds of less than 83.3 Hz.

Normalised radial load area for the actual bearing, for the various rotational speeds and radial loads and calculated according to Eq. (2), is shown in Fig. 6.

As expected, there seems to be a good correlation between relative current contact conditions (Fig. 4) and normalised radial loads (Fig. 6). This means thinner fluid film and greater wear under the combination of lower rotational speed and larger radial loads (poor hydrodynamic lubrication). In Fig. 7, the normalised radial load area is shown as a 2-D plot.

Results from the contact measurements are shown both in Figs. 4 and 8 as 3-D plots. In Fig. 8, the occurrence location of oil whirl (x) and oil whip (o) at different rotational frequencies are also plotted.

According to Fig. 8, oil whirl and oil whip did not occur at radial loads of 20 N and higher. The transition from oil whirl to oil whip takes place at a rotational frequency of approximately 83.3 Hz. Figure 8 shows no average electrical current under conditions of oil whirl or oil whip. At higher average electrical current under increasing loads, neither oil whirl nor oil whip occurs.

4 Interpretation of results

In order to determine that oil whirl and whip that can give rise to a damaging vibration level is occurring, the best start point is the use of a specific normal vibration level for the given equipment type. Moreover, when designing fluid film bearings, the limitations of the geometry of the bearing should be taken into account.

The normalised loads for the measurements are calculated by the following formula:

$$W' = \left[\frac{W}{\eta_e \cdot N \cdot b \cdot d}\right] \cdot \left[\frac{c_d}{d}\right]^2 \tag{2}$$

where

- W radial load on the bearing [N]
- η_e dynamic viscosity=0.075 Ns/m^2 at 20 °C
- N shaft rotational speed [r/s]
- b bearing width=0.015 m
- d shaft diameter in the bearing=0.025 m
- d_i inner bush diameter [m]
- c_d bearing clearance=$d_i - d$=0.000222 m
- e eccentricity [m]
- ε relative shaft eccentricity=$2e/c_d$ [−]

Calculated load capacity of a fluid film journal bearing is shown in Fig. 5, which also contains a recommended area of operation for the fluid film bearing. For a bearing of a given design, normalised load is only a function of radial load, oil viscosity and rotational speed.

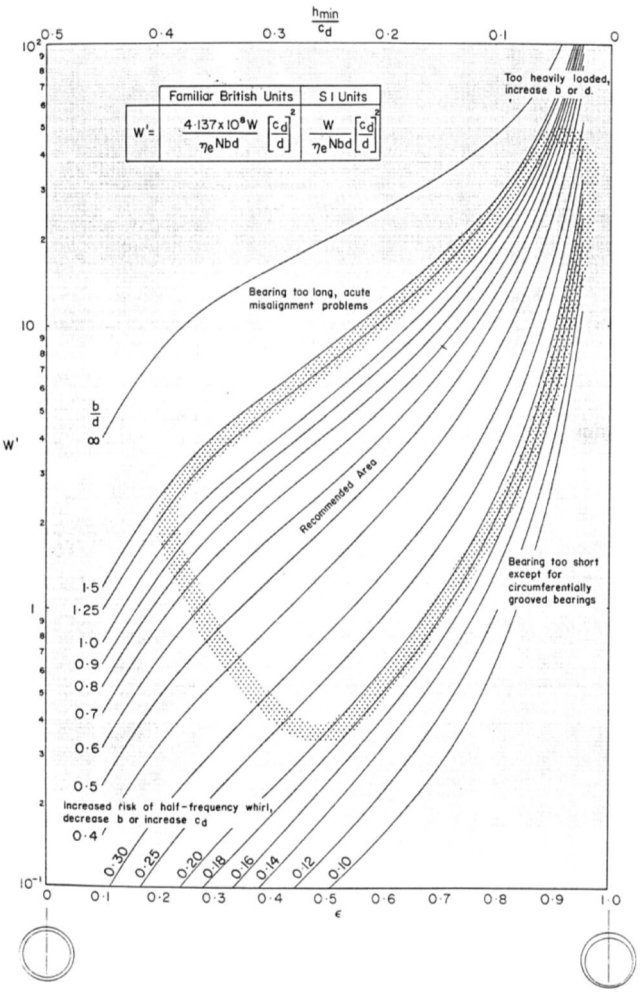

Fig. 5 Radial load capacity for fluid film bearing [3]

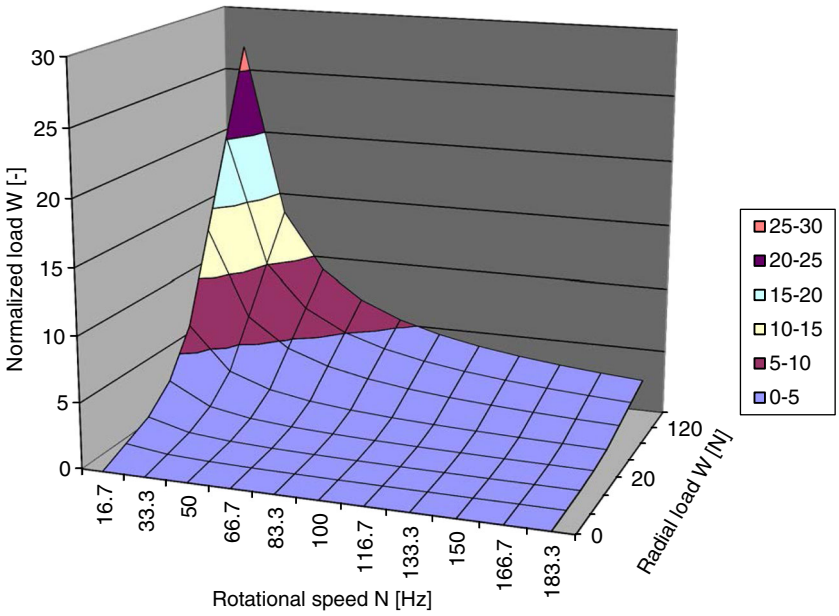

Fig. 6 Calculated normalised radial load

When the registered values of the oil whirl and oil whip, stored in a data logger with an in-built frequency analysis module, are added to Fig. 9, they lie close to the abscissas. Both Figs. 8 and 9 show 'normal' progression of relative average current contact as a function of rotational speed during increasing radial load. However, at radial loads equivalent to 120 N, relative contact higher than expected is registered at shaft rotational speeds of 33.3, 50 and 66.7 Hz. The authors found out that this may be caused by disconnected particles from the bearing surfaces: the particles periodically separate from the bearing surfaces and create short-term contacts until they are worn away, removed or their size is reduced. At rotational speeds of 16.7 Hz and lower, complete contact with the radial load equivalent to 120 N and higher may be expected. This equals a normalised load of approximately 20 (see Figs. 6 or 7). Based on Fig. 5, this corresponds to approximately 82 % of the recommended maximum load capacity for this bearing having b/d ratio of 0.6. Under the actual conditions, the real non-dimensional load will be higher than 82 % because it has been determined without allowing for the local oil viscosity; due to local heating in the bearing, it will be lower than the nominal viscosity measured at ambient temperature.

Even without using correlation analysis, it may be concluded, based on a visual comparison of Figs. 6 and 8, that there is a relation between increasing normalised load and increasing relative electrical current. However, Figs. 8 and 9 show certain variations/interference in the measurements, especially at radial loads of F=40 N and F=80 N. In addition, the measurement point (F=120 N and n=50 Hz) behaves outside of expected area as something that may be described as periodically metallic contact between the bearing surfaces due to one or more disconnected particles in the oil.

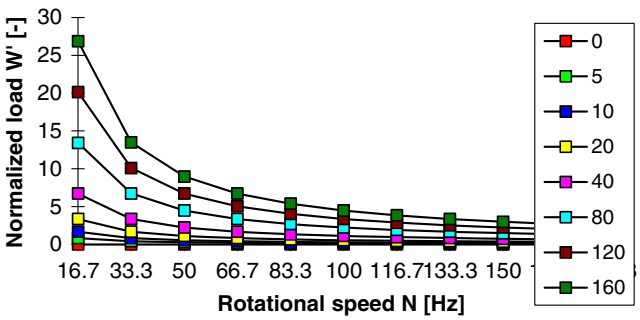

Fig. 7 Calculated normalised radial load (2-D plot)

5 Conclusion

Previous experiments using a bearing bush made of plexiglass and coloured oil showed that the bearing oil film might become invisible during oil whip. This may interpreted as a significant amount of metallic contact between the shaft and the bearing bush.

The results from the frequency analysis and from the electric current measurements of the present study do not support this. There was little or no increase in electric current in the contact surfaces of the fluid film bearing in the cases when oil whirl and oil whip appeared. On the other hand, a moderate radial load on the fluid film bearing showed a marked increase of average electric current through the oil

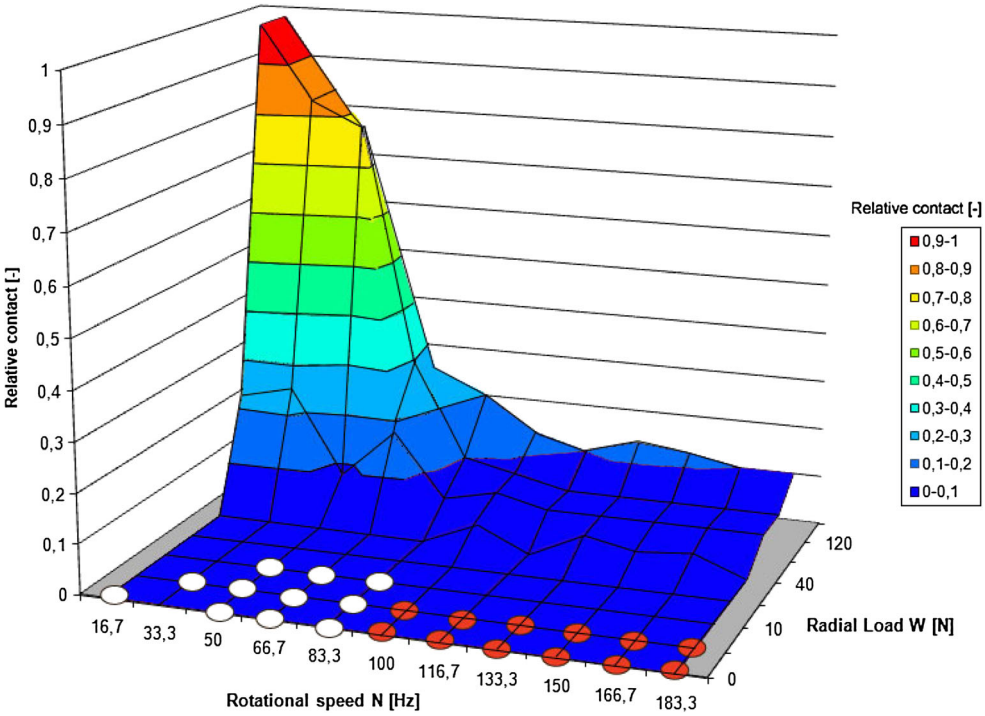

Fig. 8 Relative current contact conditions in the bearing. *White O* oil whirl conditions, *red O* oil whip conditions

film. This seems to indicate that the apparent vanishing of the oil film in the transparent bushing tests is not complete—the film is just too thin to be visually detected. This in turn strongly suggests the creation of an effective squeeze film under these conditions. Such a film may be strong enough to carry a low load but not a high one.

The above suggests that the effects of oil whirl and whip may not be as detrimental as commonly believed. The authors are not suggesting that these phenomena may be ignored. It is quite possible that small contacts are established, their total conducting area being too small for an electric current to be detected. Such local—and frequent—loads may indeed be causing wear since the local pressures may be large because of small areas involved. Long time tests should probably be conducted to investigate this possibility.

One cannot rule out that the above findings are specific to the particular bearings tested. Fluid film bearings having other dimensions should also be studied. However, we believe that bearings having parameters corresponding to values inside the

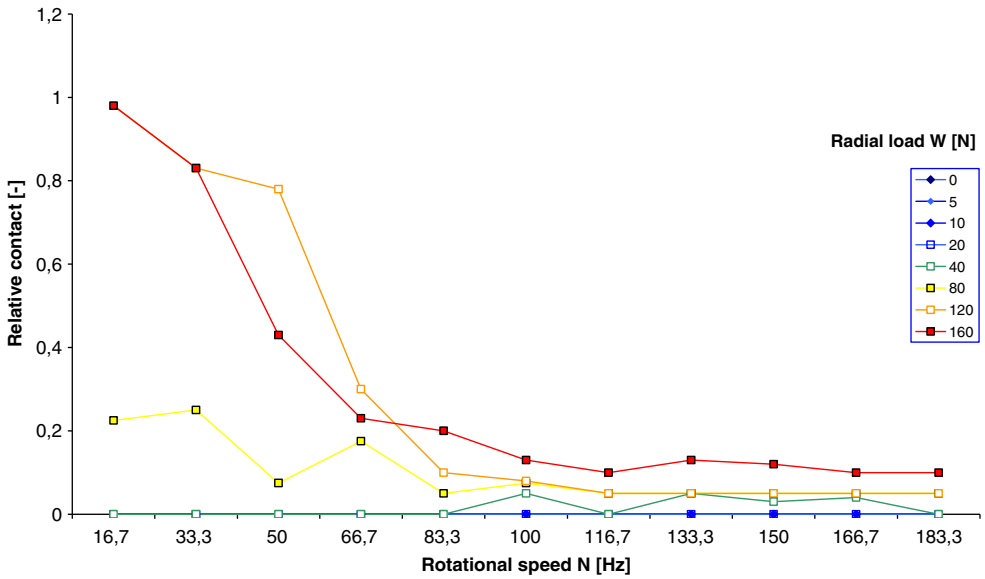

Fig. 9 Contact measurements

recommended normalised load area of Fig. 5 would show much of the same behaviour as that shown in our tests.

Summing up the above findings, we may make the following statements regarding the condition of oil whirl and oil whip: They do not always lead to fluid film breakdown. The contact area is strongly dependant on load. Under realistic conditions, the consequences seem to be less severe than commonly expected.

Acknowledgments The authors would like to acknowledge the editor and the anonymous referees for their valuable comments and suggestions which have improved the quality of the paper.

References

1. Goodwin MJ (1989) Dynamics of rotor-bearing systems. Unwin Hyman Ltd, London, pp 167–188
2. Muszynska A (1986) Whirl and whip—rotor/bearing stability problems. J Sound Vib 110(3):443–462
3. Robbersmyr KG, Olsen H (1996) On oil whirl and oil whip, vol 1. The 7th symposium of Nordic Tribology, Nordtrib 96, Bergen, Norway, pp 16–19, June 1996
4. Muszynska A (1988) Stability of whirl and whip in rotor/bearing systems. J Sound Vib 127(1):49–64
5. Fan C-C, Syu J-W, Pan M-C, Tsao W-C (2011) Study of start-up vibration response for oil whirl, oil whip and dry whip. Mech Syst Signal Process 25(8):3102–3115
6. Schweizer B (2009) Oil whirl, oil whip and whirl/whip synchronization occurring in rotor systems with full-floating ring. Nonlinear Dyn 57(4):509–532
7. de Castro HF, Cavalca KL, Nordmann R (2008) Whirl and whip instabilities in rotor-bearing system considering a nonlinear force model. J Sound Vib 317(1–2):273–293
8. Burke AE, Neale MJ, Martin FA (1966) Calculation methods for steadily loaded pressure fed hydrodynamic journal bearings, Engineering Science Data Item No. 66023, Institution of Mechanical Engineers, London
9. Berry JE (2005) Oil whirl and whip instabilities—within journal bearings, Machinery lubrication magazine, May, Issue Number: 200505
10. Yang SH, Kim C, Lee Y-B (2006) Experimental study on the characteristics of pad fluttering in a tilting pad journal bearing. Tribol Int 39(7):689–694
11. STI Field Application Note: Bearing Failure Modes, Ref.: http://www.stiweb.com/appnotes/jbfail.htm
12. IOtech: Steam turbine rotor testing using the ZonicBook, Application Note #93. Ref: http://www.iotech.com/an93.html
13. Norton RL (2000) Machine design; an integrated approach, chapter 10.5 and 10.6, 2nd edn. Prentice Hall Inc, Upper Saddle River, pp 631–646
14. Scott R (2005) Journal bearings and their lubrication, machinery lubrication magazine, June
15. SKF condition monitoring: PRISM^4 for Windows—users manual, San Diego, USA, 1996
16. First order RC circuit, Ref: www.clarkson.edu/~svoboda/eta/plots/RC.html-3k
17. http://webphysics.davidson.edu/physlet_resources/gustavus_physlets/rccircuit.html: RC Circuit